DESIGN OPTIMIZATION OF A THREE-DIMENSIONAL STRAIN SENSOR USING MULTIPHYSICS FINITE ELEMENT ANALYSIS

B.M. Evans III, M.R. Mahfouz
University of Tennessee, Department of Mechanical, Aerospace, and Biomedical Engineering, Knoxville, TN, USA
e-mail: mmahfouz@cmb.utk.edu

Abstract- **Biomedical research at the University of Tennessee's Center for Musculoskeletal Research (CMR) has been directed toward investigating the use of novel micro-electromechanical sensors (MEMS) for orthopedic applications. Arrays of sensors will be implemented to understand prosthesis loading with sub-millimeter spatial resolution in the transverse plane. The capacitance-based strain rosette will allow joint replacement component designers and researchers to understand the effects of loading, wear, and joint motions on a local scale. This rosette includes a parallel plate capacitive sensor for measuring strain in the normal direction, an interdigitated sensor for measuring strain in the plane of the sensor, and a differential capacitive sensor for measuring the strain in the plane normal to the sensor. This paper discusses the effects of strain on sensor capacitance and evaluates the effects of loading and geometry using finite element analysis for the optimization of the electrode geometries of these arrays.**
***Keywords* - MEMS, strain, pressure, sensor**

I. INTRODUCTION

Prior research in our facility using *in vivo* video fluoroscopy and digital image analysis to determine the motions of normal subjects and subjects following the total knee arthroplasty procedure has shown that the knee may have translations and rotations about all three Cartesian axes during flexion and extension. Local sliding and axial rotation of the tibia with respect to the femur is part of the natural motion of the knee [1]. Deviations of the knee replacement components from the natural motion of the knee can have a significant effect on loading, range of motion, and patient satisfaction [2].

The effectiveness of total knee arthroplasty at relieving pain and improving patient motion is widely recognized. The number of knee replacement implants surviving 10–15 years is routinely greater than 90%. It is estimated that 321,084 TKAs and 32,159 TKA revisions were performed in the United States in 2002 [3]. In a recent multi-center study of 318 patients with failed total knee replacements, it was determined that polyethylene wear was responsible for 24.5% of implant revisions [4].

Understanding the motions and loading conditions of orthopedic components is essential to improving patient motions and improving the wear characteristics of knee replacement implants. The relative implant kinematics, contact areas, and contact stresses are important to the performance and wear of any prosthesis. Maximum contact pressures between a metal total knee arthroplasty component and a polyethylene insert have been reported to approach 20 MPa (7 MPa for hip replacements) by researchers using finite element modeling, Fuji pressure sensitive film, and cadaver studies [5-8]. Recent advances in microfabrication technology have yielded the tools to create *in vivo* sensors capable of determining the contact pressure and area as well as the contact motions with minimal modification of existing biomedical components.

*This work was funded in part by Zimmer Orthopedics, Inc. Warsaw, IN.

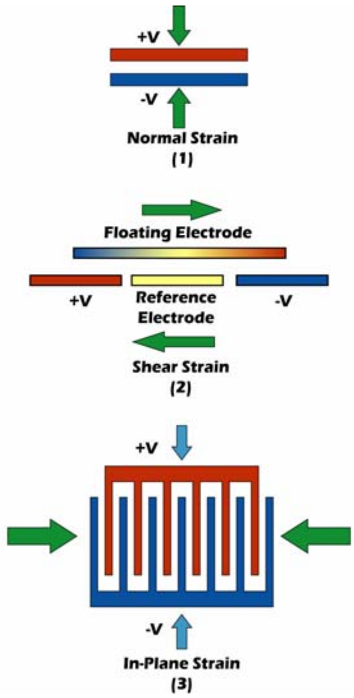

Fig. 1. Two-dimensional illustration of sensor geometry and line of action for the multi-axial strain sensor elements including the applied voltages for each sensor.

II. METHODOLOGY

We have investigated the use of three different sensors to determine the normal strain, in-plane strain, and shear strain. To fully characterize the strain tensor in three dimensions, six sensors are required to solve for the three normal strains and three shear strains. A parallel plate capacitor is used to determine the strain normal to the plane of the sensors, ε_{zz}. Two differential translating capacitors indicate the shear components out of the sensor plane, ε_{zx} and ε_{zy}. Three interdigitated capacitors function to determine ε_{xx}, ε_{yy}, and ε_{xy}. Fig. 1 illustrates the electrode configurations for these geometries.

A combination of analysis tools have been used in the design of this system. The MEMS design software Coventor (Coventor, Inc. Cary, NC) was used extensively in this

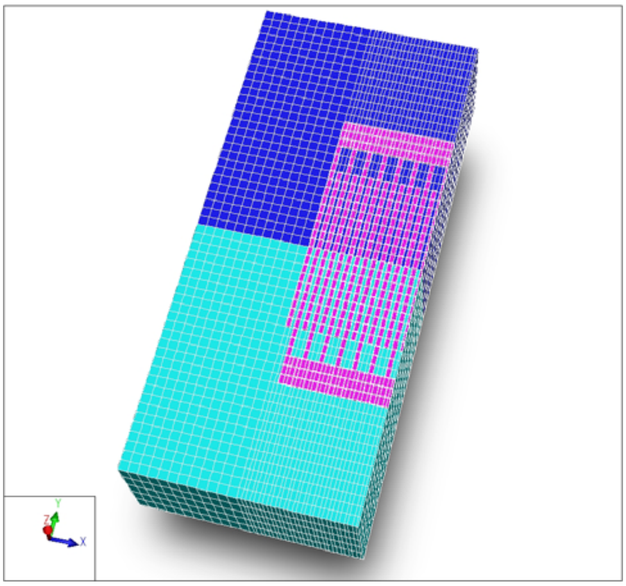

Fig. 2. Typical finite element mesh from Coventor for multi-physics modelling of electrode structures. Symmetry in the YZ plane has been used to simplify the analysis and allow for a finer mesh in the analysis region. Upper parylene and polyethylene layers are hidden for clarity.

project. Coventor is capable of 2D and 3D modeling of MEMS geometry, process simulation, and multi-physics finite element analysis. Once the design is ready for fabrication, Coventor can export the GDSII files required by most pattern generators to create masks for photolithography.

Finite element methods have been used to investigate creating a sensor array capable of fully characterizing the pressure inside implant components. The effects of stray capacitance play an important role in this project, and Maxwell (Ansoft, Inc. Pittsburgh, PA) was chosen for the investigation of fringe field effects. Each sensor was modeled with a 10 volt potential applied to the electrodes, and a unit load of 1 μN/μm (1MPa) was applied to the structures for the loading simulation.

Parabolic Manhattan brick elements were used for all Coventor models, which are 27 node quadratic elements with three nodes per edge. Coventor uses the solver from Abaqus (Abaqus, Inc. Providence, RI) finite element software for solving mechanical simulations. Linear elastic behavior was assumed for all materials in this investigation. Loads resulting in 1 MPa stresses were applied which should not violate the linear elastic assumption; however, in the actual prosthesis previous research has shown that loads may approach the yield stress of the material [5,6,8]. A typical mesh is shown in Fig. 2. The material properties of gold were used for all electrodes, and all electrodes were covered in a 2 micrometer layer of parylene and embedded in polyethylene.

Coventor uses a boundary element method to solve the Laplace equation in a single-layer for surface charge given an applied voltage. As part of this algorithm, the three-dimensional continuum element mesh is collapsed into a three-dimensional arrangement of shell or boundary elements. The MemElectro electrostatic module of Coventor uses a corrected fast Fourier transform technique to simplify the resulting system matrix. MemElectro solves the Laplace equation iteratively in a single-layer form (Gauss' Law) for the surface charge q, given an applied potential V. Because Coventor does not solve for the field in the dielectric layers, Maxwell was used for the computation and visualization of the three-dimensional fields [9].

The method for determining the change in capacitance due to the applied loads was to perform the electrostatic analysis on the model, followed by the mechanical deformation analysis due to a 1 MPa load. A second electrostatic analysis was performed on the deformed geometry. The difference between the undeformed and deformed geometry computed capacitance is the reported change in capacitance. Using this approach, convergence studies were performed on initial geometries of each electrode type. The mesh density sufficient for mesh convergence better than 0.25% was determined, and this mesh density was used for subsequent models. Typical models had between 10,000 and 25,000 elements.

For the parallel plate electrodes, one-quarter symmetry was used to reduce the computational requirements of the model. The effects of the desired load were measured as well as the effects of applying transverse and shear loads. A load sensitivity analysis was performed on the parallel plate geometry using loads ranging from 0.02-20 MPa in eight logarithmic steps. The effects of electrode size were investigated using pairs of electrodes with nominal 1, 2.5, 5, 7.5, and 10 picoFarad capacitors. The dielectric layer used in these simulations was 2 micrometers of parylene which has a dielectric constant of 2.95. For a 2 micrometer dielectric thickness, a single edge of the square electrodes measured 274, 433, 614, 751, and 848 micrometers, respectively.

As shown in Fig. 2, symmetry in the YZ plane was used to reduce the number of elements in the interdigitated sensor model. Due to operating system limitations, which only permit 2 gigabytes of ram per application, the interdigitated model was simplified based on the number of legs and the length of the legs such that sufficient convergence of mesh density was reached. The interdigitated capacitor is sensitive to the effect of strain in longitudinal (along the direction of the legs) and the lateral directions. This is apparent in the longitudinal direction as the length of the legs are stretched increasing the capacitance, and in the lateral direction as the gaps between the legs change. Studies on the geometry (leg length, number of legs, and thickness) were used to optimize the sensitivity of this sensor to a single direction.

Element two in Fig. 1 is a differential capacitor used to measure the shear strain in the material. Voltage is applied between the two outer electrodes labelled +V and –V, the upper electrode is electrically floating, and the center electrode, Vref, indicates the measurement. This arrangement has zero signal when balanced and motion of the upper plate relative to the lower ones yields a signal which has a sign indicating the direction of motion. The floating electrode becomes unbalanced and charge is induced by the lower electrodes when subjected to shear strain. As the upper plate becomes charged, the reference electrode assumes the opposite charge. This electrode arrangement has the capability of rejecting common modes of error. This is effective for both electrical noise and off-axis strain. One-half symmetry was used to model the differential sensor and the sensitivity of this configuration to shear strain and off-axis loading was investigated using the previously stated methods.

III. RESULTS

A. Normal Strain

The results of the normal strain sensor indicated that this sensor has good sensitivity to normal strains and exhibits the desired preference for this loading condition. Fig. 3 illustrates the graphical strain results from 1 MPa normal loading. Compressive strains are negative in this figure and the stresses are largest in the encapsulating polyethylene material. The change in capacitance with different electrode sizes is also shown in Fig. 4. On the secondary axis in Fig. 4, the ratio of the sensitivity of the parallel plate sensor to off-axis loads to that of normal loads ranges from 0.53 to 0.54, as compared to the Poisson's ratio of polyethylene which is 0.46. Data is shown for normal and orthogonal loading. Response in the orthogonal direction is expected due to Poisson's ratio effects. The ratio of the normal and orthogonal responses is shown on the secondary axis.

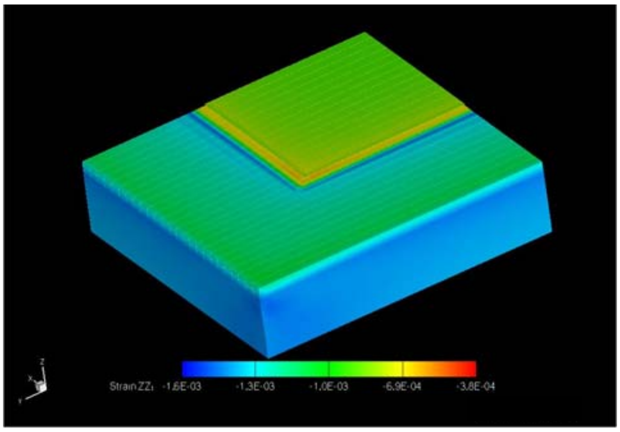

Fig. 3. Strain results of normal strain sensor.

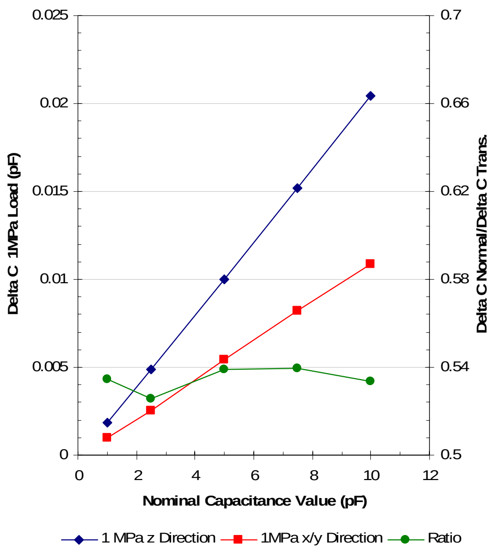

Fig. 4. Change in capacitance with 1 MPa normal loading and 1 MPa loading applied orthogonal to the normal axis. The ratio of the normal or z direction loading is plotted with circles on the secondary y axis.

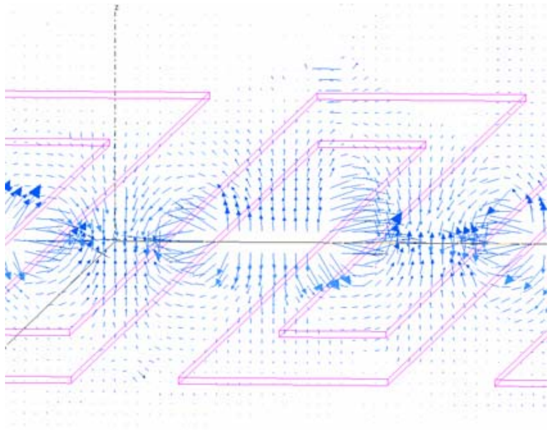

Fig. 5. Electric field vectors from Maxwell simulation of the interdigitated capacitor design.

B. In-plane Strain

For a thin-film interdigitated capacitor structure the capacitance effect from the fringe capacitance can be equal or greater to than the capacitance from the sides of the digits. This effect is seen in the Maxwell analysis of the electric field shown in Fig. 5. Results of the multi-physics Coventor modelling show that the interdigit fringe capacitance does not change as significantly from loading orthogonal to the axis of the digits as the normal wall capacitance. This effect is also illustrated in the plots of Fig. 6, which show how the ratio of the change in capacitance with longitudinal loading to orthogonal loading approaches the desired value of Poisson's ratio with increased electrode thickness. Structures in this analysis consisted of 15 interdigitated electrodes that were 150 micrometers long and 4.75 micrometers wide with 2.25 micrometer gaps. Actual structures have more digits of longer length. Results from previous analyses have shown that the change in capacitance scales linearly with number of electrodes and electrode length.

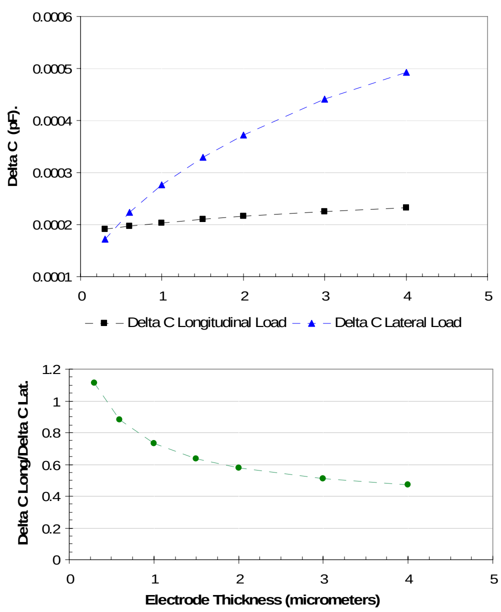

Fig. 6. Effect of electrode thickness on interdigitated electrode response to in-plane strain.

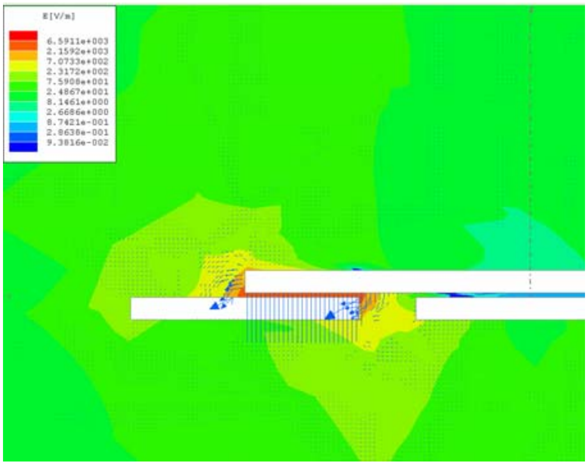

Fig. 7. Enlarged view of shear sensor electrodes showing electric field from Maxwell analysis. Only half of the sensor is visible.

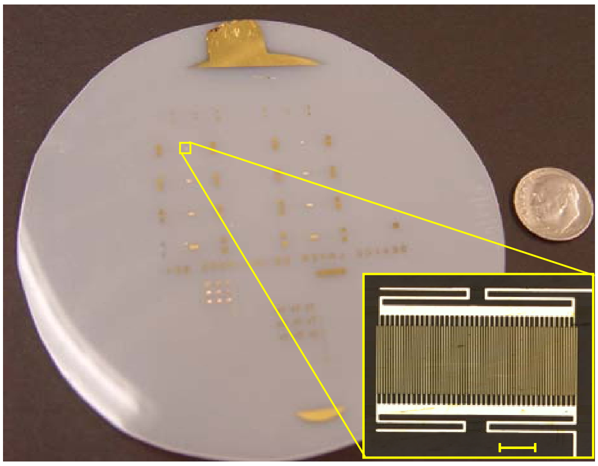

Fig. 8. Example of electrodes fabricated on biocompatible polymer surface. Substrate is high density polyethylene and the dielectric material is parylene.

C. Shear Sensor

The lower shear sensor electrodes were 1,050 micrometers in length and 100 micrometers in width. The upper floating electrode was 1,000 micrometers in length and 270 micrometers in width. The shear sensor was modeled using one-half symmetry to reduce computational requirements. The boundary conditions for this model were as follows: a floating potential (zero net charge) boundary condition was applied to the upper floating electrode, +5 volts was applied to one of the lower, outer electrodes while -5 volts was applied to the electrode, and a potential of 0 volts was applied to the center reference electrode. This sensor will be made more compact using an interdigitated lower structure in future designs. Results of the Maxwell field analysis are shown in Fig. 7 above.

Initial devices have been fabricated using all biocompatible materials, and the biocompatible polymer parylene has been processed using photolithography and reactive ion etching to produce patterns of polymer features. Fig. 8 illustrates our research toward fabricating electrodes using fully biocompatible processes. Ongoing work on designing application-specific integrated circuits (ASICS) that are incorporated into the implant and that can measure the small changes in capacitance is also underway. Initial sets of sensors have been fabricated and testing of these has been initiated. These biocompatible sensors will give researchers better understanding of the kinetics and kinematics of orthopedic components.

IV. CONCLUSIONS

A sensor array has been designed that will allow for the full characterization of stress and strain in three dimensions. Optimization of this system has been necessary to improve the performance and reduce the effects of off-axis loads. Finite element analysis has shown that the parallel plate sensor responds to applied stress in a linear manner with increasing load and that the application of off-axis loads results in a response that is in accordance with the expected Poisson's ratio deformation. Analysis of the interdigitated sensor for in-plane strains has shown that increasing the change in capacitance with applied load increases linearly with increasing leg length and by increasing the number of legs. The response to loads applied in the direction of the legs or orthogonal to the legs can be "tuned" primarily by increasing the thickness of the electrodes and to some extent by changing the width of the electrode digits and the gap between them. A capacitance-based shear sensor has been analyzed that has built-in rejection of displacements that are in the intended shear direction, and initial finite element results of this sensor look promising.

REFERENCES

[1] R.D. Komistek, D.A. Dennis, M.R. Mahfouz, "In Vivo fluoroscopic analysis of the normal human knee," *Clin. Orthop. Relat. Res.* vol. 410, pp. 69-81. May 2003.

[2] S.Y. Lee, N. Matsui, M. Kurosaka, R.D. Komistek, M.R. Mahfouz, D.A. Dennis, S. Yoshiya, "A posterior-stabilized total knee arthroplasty shows condylar lift-off during deep knee bends," *Clin. Orthop. Relat. Res.* vol. 435, pp. 181-185. June 2004.

[3] R. Kane, K. J. Saleh, T. Wilt, B. Bershadsky, W. Cross, R. MacDonald, I. Rutks, "Total knee replacement," Rockville, MD: Agency for Healthcare Research and Quality. 2003. AHRQ Publication No. 04-E006-2.

[4] K.J. Mulhall, H.M. Ghomrawi, S. Scully, J.J. Callaghan, K.J. Saleh, "Current etiologies and modes of failure in total knee arthroplasty revision," *Clin. Orthop. Relat. Res.* vol. 446, pp. 45-50. May 2006

[5] J.P. Halloran, et al., "Explicit finite element modeling of total knee replacement mechanics," *J. Biomechanics*. vol. 28, pp. 323-331. 2005

[6] W. Rostoker, J.O. Galante, "Contact pressure dependence of wear rates of ultra-high molecular weight polyethylene," *J. of Biomaterials Research.* vol. 13, pp. 957-964. 1979

[7] D.D. D'Lima, J.C. Hermida, P.C. Chen, C.W. Collwell, "Polyethylene wear and variations in knee kinematics," *Clin. Orthop.* vol. 392, pp. 124-130. 2001

[8] H. Ishikawa, H. Fujiki, K. Yasuda, "Contact Analysis of Ultrahigh molecular weight polyethylene articular plate in artificial knee joint during gait movement," *J. Biomech. Eng.* vol. 118, pp. 377-386. 1996.

[9] Coventor software reference manual. Coventor, Inc. Cary, NC.